Cellulose (2026) 33:3833–3852
https://doi.org/10.1007/s10570-026-07021-3

ORIGINAL RESEARCH

Counterion condensation, ion pairing and scattering properties of carboxymethyl cellulose with mono- and di-valent ions

Elmira Abbasi GharehTapeh · Takaichi Watanabe · Ferenc Horkay · Can Hou · Carlos G. Lopez · Max Hohenschutz

Received: 10 June 2025 / Accepted: 20 March 2026 / Published online: 26 April 2026
© The Author(s) 2026

Abstract We study the scattering and conductometric properties of a semiflexible polyelectrolyte, carboxymethyl cellulose (CMC), with monovalent and divalent counterions in aqueous media without added salts. The scattering patterns for the magnesium salts of CMC display a broad shoulder instead of the scattering peak observed for the monovalent salts. This suggests weaker electrostatic repulsion between chains and a consequent loss of local order. The result is consistent with conductivity measurements, which reveal that the effective charge of the backbone for MgCMC is approximately half that of NaCMC. The decrease in charge density agrees with Oosawa–Manning condensation, which expects the charge density to be inversely proportional to the counterion valence. Alkali metal counterions show large differences in ion-pair formation but only a weak effect in counterion condensation. We suggest that paired ions are a subset of condensed ions. A review of different methods to evaluate counterion condensation, including potentiometry, osmometry and viscosity-based methods is presented. Qualitative agreement between these methods is found and possible reasons for the discrepancies are discussed.

Keywords Polyelectrolyte · Counterion condensation · Carboxymethyl cellulose · SAXS · Conductivity · Ion pairing

Ferenc Horkay: Deceased.

Supplementary Information The online version contains supplementary material available at https://doi.org/10.1007/s10570-026-07021-3.

E. A. GharehTapeh · C. G. Lopez (✉)
Materials Science and Engineering Department, The Pennsylvania State University, 80 Pollock Rd, State College, PA 16802, USA
e-mail: cvg5719@psu.edu

T. Watanabe
Department of Applied Chemistry, Graduate School of Environmental, Life, Natural Science, and Technology, Okayama University, 3-1-1 Tsushima-naka, Kita-ku, Okayama 700-8530, Japan

F. Horkay
Section on Quantitative Imaging and Tissue Sciences, Eunice Kennedy Shriver National Institute of Child Health and Human Development, National Institutes of Health, Bethesda, MD 20892, USA

C. Hou · M. Hohenschutz (✉)
Institute of Physical Chemistry, RWTH Aachen University, Landoltweg 2, 52074 Aachen, Germany
e-mail: hohenschutz@pc.rwth-aachen.de

Introduction

Ion-polymer interactions play a central role in many biological processes including protein folding, DNA condensation and the origin of life (Pineda et al. 2024; Agrawal et al. 2024; Tasaki 2012; Verdugo 2005; Sircar et al. 2013; Wnek 2016). Specific ion binding can stabilize folded conformations in proteins

or alternatively promote their aggregation. In the case of nucleic acids, multivalent cations such as Mg^{2+} and spermidine induce DNA condensation by neutralizing backbone charges and promoting intermolecular association. Despite the central importance of charged polymers to biological systems, our understanding of ion-containing polymers in solution lags far behind that of neutral polymers. This is the result of the larger number of experimental variables that must be studied and the long-ranged nature of electrostatic forces, which are difficult to treat theoretically (Dobrynin and Rubinstein 2005; Lopez et al. 2024).

Condensation and binding

Two concepts are commonly used to describe polyion–counterion interactions. The first is counterion condensation, which refers to the accumulation of counterions in the vicinity of the backbone due to electrostatic attraction from the polyion. The condensed counterions do not contribute to the osmotic pressure of the solution or to transport properties such as electrical conductivity. The second concept is ion-pairing, which occurs when the counterion comes in close contact with the ionic group of the polyelectrolyte. What qualifies as a close contact is difficult to demarcate, and different ideas have been put forward (Marcus and Hefter 2006; Gregory et al. 2022). The solvent in the close vicinity of an ion experiences a huge pressure from the electrostatic field and as a result its density increases, a phenomenon known as electrostriction. When an ion-pair forms, some of the electrostricted solvent is released, leading to a volume increase. This provides a functional definition for ion-pair formation (Hemmes 1972).

Understanding counterion condensation is important because virtually all solution properties are influenced by the effective charge of the chain. Ion-pairing does not influence many macroscopic solution properties, but it plays a crucial role in applications such as ion-recovery processes and in coacervation (Strauss and Ross 1959; Danielsen et al. 2020; Sing and Qin 2023).

Oosawa–Manning (OM) condensation

When a polyelectrolyte dissolves in a solvent, a fraction of the counterions dissociate from the backbone and the rest stay in the close vicinity of the chain's backbone, thereby lowering the effective polyion charge (Essafi et al. 1999; Matsumoto et al. 2022; Tang and Rubinstein 2022; Muthukumar 2004). One of the first successful attempt to describe this phenomenon, known as counterion condensation was the theory of Oosawa and Manning (Oosawa 1957, 1971; Manning 1969). In their model, an infinite, isolated rod-like polyelectrolyte is considered. Counterions are treated as point-like charges interacting via Debye–Hückel screened potentials and the backbone as possessing a uniform charge density. Under these (and other) assumptions, the famous result is obtained that monovalent counterions will condense onto the backbone until the effective charge is reduced to one charge per Bjerrum length (l_B), with:

$$l_B = \frac{e^2}{k_B T 4\pi\epsilon} \tag{1}$$

where e is the electrostatic unit of charge, ϵ the dielectric constant, k_B is Boltzmann's constant and T the absolute temperature.

The critical charge on the chain is predicted to be:

$$\mu_{eff} = \frac{e}{z l_B} \tag{2}$$

where z is the valence of the counterion. This means that when the bare charge of a chain (the charge of the backbone without counterions) exceeds μ_{eff}, counterions will bind or condense onto the chain until the effective charge of the chain (i.e. the sum of the charge of the backbone and the neutralising counterions) decreases to $e/(l_B z)$, that is one charge per Bjerrum length for monovalent counterions and one charge per two Bjerrum lengths for divalent counterions. For higher-valent counterions, specific ion effects are usually strong, and treatments based on Debye–Hückel screening are not appropriate (Lopez et al. 2024; Ehtiati et al. 2022; Smiatek 2020).

Counterion condensation is often discussed in terms of the coupling parameter (u), which is the ratio between the Bjerrum length and d, the distance between ionic groups along the backbone ($u = l_B/d$). The Manning model predicts counterion condensation to set in when u exceeds a value of 1 for monovalent ions or 2 for divalent ones. A useful way of experimentally quantifying counterion condensation is to measure their activity using ion-selective electrode potentiometry. The theory of Manning predicts

for the activity coefficient of polyelectrolytes with monovalent counter-ions in salt-free solution:

$$\Gamma = \begin{cases} e^{-u/2} & \text{if } u < 1 \\ \frac{1}{\sqrt{eu}} & \text{if } u > 1 \end{cases} \quad (3)$$

and for divalent counterions (Manning 1972):

$$\Gamma = \begin{cases} e^{-u} & \text{if } u < \frac{1}{2} \\ \frac{1}{2\sqrt{eu}} & \text{if } u > \frac{1}{2} \end{cases} \quad (4)$$

Note that according to Eqs. 3 and 4, the activity of the free counterions is lower than their concentration.

The Oosawa and Manning models are derived for rigid and isolated chains (i.e. rod-like polyelectrolytes at infinite dilution). Its extension to higher concentrations results in more complex behaviour (O'Shaughnessy and Yang 2005; Oosawa 1971). Experimental evidence on flexible polyelectrolytes (Wandrey 1999; Wandrey et al. 2000) show that below the overlap concentration counterion dissociation increases upon dilution, approaching the no-condensation limit at infinite dilution, in agreement with later simulation results (Liao et al. 2003) and contradicting the Oosawa–Manning model. Interestingly, the OM model appears to hold in the semidilute regime.

A complication that arises when applying the Oosawa–Manning model to flexible or semiflexible polyelectrolytes is that, because unlike for the case of rigid chains, the conformation of the chain may depend on the effective charge of the backbone, thus requiring a more involved calculation where the free energy of the chain and the counterions are calculated self-consistently (Muthukumar 2004). Further, interactions between counterions and polymers include effects arising from sharing of hydration shells and ion-pair formation, not accounted for in the Oosawa–Manning theory (Lytle et al. 2021; Marcus and Hefter 2006).

The effective charge of the polyelectrolyte backbone influences many solution properties, including the chain conformation (Nova et al. 2025), screening lengths (Nishida et al. 1995), charge transport (Diederichsen et al. 2019; Kondou et al. 2023; Marioni et al. 2024), osmotic pressure (Colby 2010), and phase behaviour (Lopez et al. 2024; Chen et al. 2021). Therefore, it is of interest to understand how counterion condensation depends on the nature of the solvent, polymer and counterion.

Here we investigate how the properties of the counterion influence the degree of condensation for semiflexible polyelectrolyte carboxymethyl cellulose (CMC), an extensively studied anionic cellulose ether (Jimenez et al. 2020, 2022; Różańska et al. 2019; Behra et al. 2019; Arumughan et al. 2023; Wagner et al. 2023; Legrand et al. 2024; Yoshida et al. 2024). NaCMC finds many applications as a thickener, moisture retainer and structuring agent in pharmaceutical, food, wine, cosmetic and other formulations (Kim et al. 2022; Wang et al. 2024; Liu and Zhao 2019; Hou et al. 2024b; Kong et al. 2024; Zhang et al. 2022, 2024; Cai et al. 2025; Sommer 2025). While carboxymethyl cellulose is normally employed as a sodium salt, formulations containing NaCMC often contain divalent ions or come in contact with them when they are diluted with tap water. The interaction of divalent ions with polyelectrolytes is more complex than that of monovalent ions due to ion-specific effects (Horkay and Douglas 2025; Mussel et al. 2019; Beyer and Holm 2024; Chang and Yethiraj 2003; Glisman et al. 2024). Here we focus on the Mg^{2+} ion, which displays weak specific-ion interactions with carboxylate groups of CMC (Sharratt et al. 2020, 2021).

Activity of CMC counterions

Literature results for the activity coefficient of NaCMC and MgCMC are compiled in Fig. 1. All data were obtained using ion-selective potentiometry. The theory of Manning (Eqs. 3 and 4), shown as lines, under-predicts the activity coefficient for both monovalent and divalent salts of CMC over the entire charge density range studied.

In interpreting the data in Fig. 1 it should be noted that the distribution of substituents along the CMC backbone is not homogeneous. The degree of heterogeneity depends on the synthesis procedure used. For reference, the data of Kono et al. (2016a, b) for NaCMC synthesised via the slurry process show that for degree of substitution (DS) of 0.7, or equivalently $u \simeq 1$, corresponding to the lowest charge density in Fig. 1, there exist $\simeq 5\%$ of monomers with two carboxymethyl groups and an equal percentage with three substituted groups. Such substitution patterns are expected to display greater condensation than homogeneous ones because regions with high

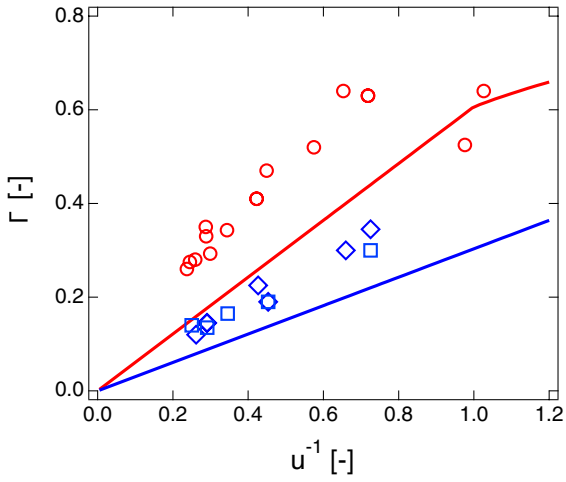

Fig. 1 Counterion activity of carboxymethyl celluloses with different degrees of substitution as a function of the charge coupling parameter. Lines are predictions of the Manning model (Eqs. 3 and 4). Data are from Rinaudo et al. (1973), Rinaudo and Milas (1971, 1974, 1975, 1978), Rinaudo (1973), Nagasawa and Kagawa (1957). Red points are for NaCMC and blue points are for MgCMC (squares) or CaCMC (diamonds)

substitution coexist with regions of low substitution. For very high DS, where the average charge spacing is much lower than l_B, heterogeneity in substitution is not important because having two adjacent charges separated by more than l_B becomes highly improbable. For such samples, Manning's theory is expected to work best. In fact, Fig. 1 shows the opposite result, with the Manning prediction agreeing with low substitution samples but underpredicting the activity of the highly substituted ones. We conclude that the agreement for low DS (high u^{-1}) samples is likely accidental.

Ion specificity and counterion binding

Beyond charge condensation, the size, electronic structure and hydration of an ion make the binding to an oppositely charged group ion-specific. For monovalent ions, such as Li^+, Na^+ or Cs^+, binding correlates with the size of the ion according to Collins' concept of matching water affinities (Vlachy et al. 2009; Collins 2004). According to Collins' concept, at small and strongly hydrated carboxylate groups such as in CMC, small ions, such as Li^+, are expected to bind most strongly due to a match of hydration water in contrast to large Cs^+, which should bind less strongly due to a hydration mismatch.

Evidence for the Collin's concept is found for the alkali metal salts of CMC in the ultrasound absorption studies of Zana and co-workers: When a counterion forms an ion-pair with the side group on the polymer, electrostricted water is released, leading to a change in volume (Tondre and Zana 1971, 1972; Zana and Tondre 1974a, b; Zana 1975; Koda et al. 2004). Ultrasound absorption is sensitive to processes which generate volume changes and thus can be used to track the strength of ion-pair formation in polyelectrolyte solutions. Counterion condensation does not usually involve a volume change and therefore does not show up in ultrasound absorption spectra, see Komiyama et al. (1974, 1976), Tondre and Zana (1975) and Tondre et al. (1978). Figure 2a plots the excess ultrasound absorption of HCMC (DS = 2.49) solutions with respect to water ($\delta\psi$) as a function of degree of neutralisation with various hydroxides. The black arrow marks $i = 0.26$, corresponding to $u \simeq 1$, the onset of OM condensation. For $i \lesssim 0.26$, $\delta\omega$ is independent of degree of neutralisation and counterion type, as expected because below the condensation threshold, no site-binding occurs. At higher degrees of neutralisation, the smaller counterions give rise to higher ultrasound absorption, indicating stronger ion-pair formation. Owing to its large size, it is often assumed that TMA^+ does not site-bind to the CMC backbone. Further assuming that replacing sodium by tetramethyl ammonium (TMA) counterions does not change the viscoelastic relaxations of the CMC solutions, the difference in ultrasound absorption between NaCMC and TMACMC solutions ($\Delta\Psi_{TMA}$) can be used as a direct measure of site-binding strength. $\Delta\Psi_{TMA}$ is plotted as a function of DS multiplied by the degree of ionisation (i) in Fig. 2b, where it is observed that data follow a linear relationship which intercepts the abscissa at iDS $\simeq 0.67$, corresponding to $u \simeq 1$. These data provide evidence that site-binding via ion-pair formation does not take place in the absence of counterion condensation.

For divalent ions, the Collins concept breaks down, as the electronic structure of the divalent cation allows for complexation and chelation with an ionic ligand, such as carboxylate. The Irving-Williams series describes the differences in relative stability of aqua complexes for divalent transition metal ions. For divalent cations, the ease of removing an aqua

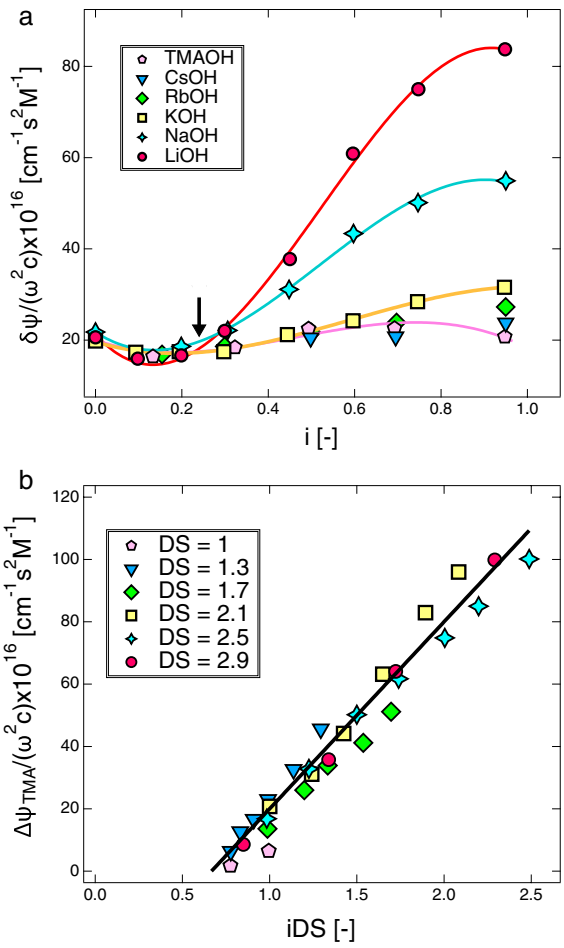

Fig. 2 Ultrasound absorption properties of CMC polymers. **a** excess ultrasound absorption with respect to water at a frequency of $\omega = 5.04$ MHz for HCMC with DS = 2.49 and $c = 0.1$ M neutralised to different degrees with TMA or alkali metal hydroxides. The black arrow indicates the point at which the distance between ionised groups is equal to the Bjerrum length ($u \simeq 1$). Lines are guides to the eye. **b** difference in ultrasound absorption of HCMC neutralised with NaOH with respect to the same polymer neutralised with TMAOH ($\omega = 2.8$ MHz). The DS of the various polymers are indicated on the legend. Line is a guide to the eye. Data are from Milas (1974) and Zana et al. (1971)

ligand is considered the main factor, while the properties of the ionic ligand, such as carboxylate, surprisingly do not play a role. Experimental results on the strength of binding of divalent metal ions to partially neutralised CMC by Rinaudo and Milas (1974) display different trends than expected from the Irving-Williams series. Both the Collins' concept and the Irving-Williams series are useful tools to understand ion-specific binding. However, deviations from them are commonly observed (Kherb et al. 2012).

Influence of ion type and valence on chain conformation

Studies on the influence of ion type on the thermodynamics of ion binding to polyelectrolytes are abundant. The influence of ion type on solution structure has received less attention (Dubois and Boué 2001; Combet et al. 2005, 2011; Hotton et al. 2023; Chremos and Douglas 2016, 2017, 2018). With some exceptions (Hotton et al. 2024), the nature of counterion type for monovalent ions is found to have a small influence on the structural (Kaji et al. 1984; Zhang et al. 2001) and dynamic (Lopez and Richtering 2019; Lopez et al. 2021) parameters of solutions. For example, the overlap concentration of CMCs with different divalent ions and of PSS with sodium and tetraalkyl-ammonium ions were found to be insensitive to ion type, indicating that the dilute chain size remains unchanged (Lopez and Richtering 2019; Gulati et al. 2024). Kaji reports a weak dependence of the correlation length of PSS solutions with H^+ and alkali metal counterions (Kaji et al. 1984). The weak influence of counterion type (for a fixed counterion valence) on conformation and dynamics contrasts with large differences observed for the binding constants in equilibrium dialysis (Hen and Strauss 1974). This suggests that competitive binding of ions is influenced by site-binding strength. On the other hand, counterion condensation, which dictates the effective charge of the backbone and thereby the conformational and dynamic properties of chains may be largely insensitive to site-binding strength.

Based on the above discussion we hypothesize the OM condensation threshold applies to CMC with various counterions and that ion-specific effects should not have a strong influence on counterion condensation.

Materials and methods

CMC polymers

Sodium salts of CMC were purchased from Sigma Aldrich (S1–S7) or donated (S8–S10) by KelcoCP or Dow. Several of these samples were characterised in

Table 1 Sample properties for different polymers used

Polymer	DS	Notes
S1	1.3	Sample 240k in Lopez (2020), see also Lopez and Richtering (2019), Sharratt et al. (2020) and Gulati et al. (2024)
S2	0.97	Same as polymer in Hou et al. (2025), conductivity and SAXS data reported in Hou et al. (2025)
S3	0.72	Same as polymer in Lopez and Richtering (2021)
S4	0.73	Sample CMC85k in Lopez (2020), DS was evaluated for this study
S5	0.81	Sample CMC94k in Lopez (2020)
S6	0.78[a]	
S7	1.4	
S8	0.87	WALOCEL-CRT 15000 PPA , donated by Dow
S9	0.79	Cekol-2000A, donated by CP Kelco
S10	0.92	Cekol-30000A, donated by CP Kelco

The molar mass of an average repeating unit is 162 g/mol + DS x 80 g/mol for NaCMC and 162 g/mol + DS x 69 g/mol for MgCMC

[a]Value obtained from manufacturer's certificate of analysis

previous studies, as noted in Table 1. The DS was determined (either in this study or in our prior works) by back titration of HCMC, where the acid is prepared by dialysis as described in Lopez and Richtering (2019), and not by alcohol wash method because the latter can yield artificially low DS values for highly substituted samples (Hedlund and Germgård 2007). The exception was S5, for which the DS value from the certificate of analysis provided by Sigma-Aldrich was used. Sodium salts were purified by dialysis against DI water until the conductivity of the bath reached a stable value of 2–3 µS/cm after at least 6 h of dialysis. The magnesium salts were prepared by addition of ×20 molar excess $MgCl_2$ to a CMC solution followed by extensive dialysis against DI water. Alkali metal salts of CMC were prepared by neutralising dry HCMC with the corresponding hydroxide to pH > 12 followed by dialysis against DI water. All samples were freeze dried after dialysis. The molecular weights of polymers S1–S5 were evaluated in earlier work, from static light scattering or intrinsic viscosity measurements, see Table 1.

Electrical conductivity

Two setups were used: One setup is the same as that described Hou et al. (2025), whereby a SevenMulti Dual pH/conductivity meter (Mettler Toledo) was used, with the probe inserted into a 10 mL centrifuge vial containing roughly 3 mL of the sample solution, which was placed in a temperature-controlled water bath and kept at 25 °C. The second setup used a SevenExcellence pH/conductivity meter (Mettler Toledo). An InLab 741 conductivity probe with 2 steel poles with an integrated temperature sensor were used to measure the conductivity over the 0.001–500 µS/cm range. InLab710 conductivity cell with 4 platinum poles were also used, measuring the conductivity through the range of 0.01–500 mS/cm. Samples in the conductivity overlap range (100–500 µS/cm) were measured by both probes to confirm the consistency of the results. The InLab 741 probe was calibrated using 100 µS/cm standard solution placed inside a water bath to equilibrate to 25 °C. The InLab710 conductivity cell was calibrated in the same manner using a 1413 µS/cm standard solution.

Small angle X-ray scattering (SAXS)

Synchrotron SAXS experiments were carried out at the SPring-8 facility in Hyogo, Japan (Beamline BL40). Samples were loaded into 2 mm capillaries. The X-ray energy was set to 12.2 keV for all measurements. Sample scattering and transmission measurements were carried out simultaneously. Radial averaging and capillary subtraction were carried out using standard procedures. For the synchrotron samples, we report data in arbitrary units. In-house SAXS measurements were performed on a NanoInXider by Xenocs. Borosilicate capillaries from WJM Glass were used as sample containers. The magnitude of the scattering vector q was calibrated using Silver Behenate and the scattered intensity was corrected by dark noise, sample transmission and capillary thickness. The reduced intensity for in-house

Table 2 Equivalent conductances of counterions in water. Data from Robinson and Stokes (2002) and Adamson (1979)

Ion	λ_C (mS/M)
Li^+	38.7
Na^+	50.1
K^+	73.5
Cs^+	76.8
Mg^{2+}	53.05

The equivalent conductance is the limiting conductance divided by the ion charge

samples shows a peak at $\simeq 0.8$ Å^{-1}, which arises from the Kapton window below the sample stage, which we are unable to fully subtract. Amorphous graphite was used as a reference standard to bring the intensities to absolute scale. Sample thicknesses were measured using a micrometer.

Small angle neutron scattering (SANS)

Neutron scattering experiments were carried out at the SANS30G beamline of the NIST research reactor ($0.0034 < q/$ Å$^{-1} < 0.4$) and the D11 beamline of the ILL, Grenoble, ($0.0022 < q/$Å$^{-1} < 0.45$). Samples were loaded into quartz cuvettes and data were reduced into absolute units using the standard procedure provided by the facility. The SANS data listed in the SI have been reduced subtracting only the cell and not the solvent contribution.

Thermogravimetric analysis (TGA)

Thermogravimetric analysis was carried out with a Discovery TGA 550 with a nitrogen flow of 50 mL/min. Relatively small masses of CMC samples (6 ± 2 mg) were loaded onto clean, tared 100 µL platinum TGA pans without lids. The samples were heated to 120 °C and held for 1 h and were then heated from 120 to 420 °C at a rate of 10 °C/min. The water content fo the CMC was evaluated from the mass loss at the first stage (25–120 °C).

Measurements were performed at $T = 25$ °C unless otherwise indicated. Scattering and conductivity data are tabulated in the supporting information.

Results and discussion

All equations use c in number of repeating units per unit volume, following the literature convention. The repeating unit or monomer is taken to be the glucose unit. When quoting values in the text, we use the more convenient units of mol/L (M). The symbol C is used to refer to concentrations in mass per volume or weight percent.

Small angle scattering

SAXS curves for MgCMC were measured for samples S1–S4 and S6–S10. SAXS data for the sodium salts of samples S1 and S2 were reported in earlier studies (Gulati et al. 2024; Hou et al. 2024a; Sharratt et al. 2020). SANS data for sample S1 was reported in Gulati et al. (2024) and Sharratt et al. (2020) and additional measurements for the same polymer in the sodium and magnesium forms are reported here. We include earlier ξ measurements for three samples with DS between 0.7 and 1.2 studied in Lopez et al. (2015, 2018). These polymers were not part of this study.

The scattering profiles of NaCMC in DI water, whether measured by SANS or SAXS showed clear correlation peaks (Horkay and Hammouda 2008; Dobrynin et al. 1995) over the entire concentration range studied, in agreement with earlier studies (Lopez et al. 2015, 2018; Sharratt et al. 2020; Gulati et al. 2024; Hou et al. 2024a). By contrast, the magnesium salts of CMC did not display correlation peaks, irrespective of DS or polymer concentration. Instead, a broad 'correlation shoulder' is observed. This feature is reminiscent of the scattering profiles observed for sodium hyaluronate in DI water solutions (Salamon et al. 2013) or polyelectrolytes with modest concentrations of added salts (Spiteri 1997; Sharratt et al. 2020; Nishida et al. 2002; Prabhu et al. 2003; Slim et al. 2022) A comparison between the scattering profiles of NaCMC and MgCMC solutions at $C = 2$ wt% is shown in Fig. 3. The concentration in units of repeating units per volume is $\simeq 5\%$ higher for the MgCMC solution. For some samples at low concentrations, a very broad peak in the high-q region appears, see for example the 1.77 g/L curve in Fig. 4. This same feature was observed in earlier study for NaCMC, but the origin was not understood (Lopez et al. 2015). Given the relatively weak electrostatic correlations in MgCMC, this appears unlikely to be a second order correlation

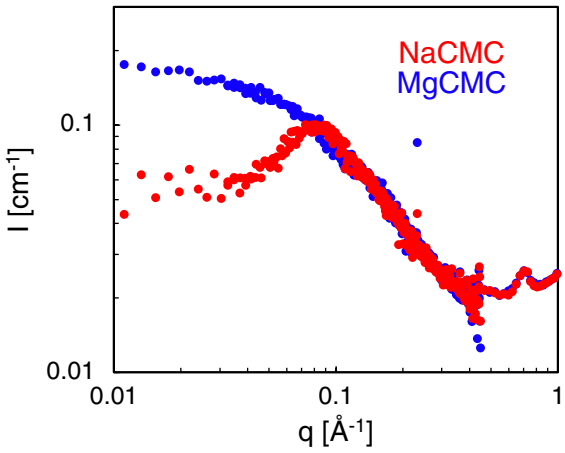

Fig. 3 Comparison of SAXS curves for sodium and magnesium salts of a solution of sample S2 in DI water. Both solutions are at a concentration of 2 wt%. The data have been binned (3 to 1) for clarity. Data are measured on the in-house instrument

peak and instead it may arise from the chain's form factor, for example due to local curling of the chain into a helical structure.

Following the approach in Salamon et al. (2013), Gulati et al. (2024) and Hou et al. (2024a), we identify the cross-over between the high-q and intermediate q as the 'shoulder position'. We fit power-laws to the high-q and medium-q regions:

$$I(q) = \begin{cases} A_1 q^{m_1} & \text{if } q \lesssim q^* \\ A_2 q^{m_2} & \text{if } q \gtrsim q^* \end{cases} \tag{5}$$

where A_1, A_2, m_1 and m_2 are used as fit parameters and q^* is the wave-vector at which the two power-laws intersect. Examples of such fits to the magnesium salt of S1 at different polymer concentrations are shown in Fig. 4. The range over which the intermediate and high-q power laws were fit was identified visually, values for the various parameters are tabulated in the supporting information. Note that at high concentrations, the influence of the low-q upturn (Ermi and Amis 1998; Lopez et al. 2024) on the mid-q scattering region becomes more important, which makes the power-law fits less reliable.

The variation of the two exponents with concentration for the various MgCMC samples studied is plotted in Fig. 5. The values of m_1 and m_2 for each polymer sample studied are listed in the supporting information. The observed values are similar to those reported for flexible polyelectrolyte sodium polyacrylate (Nova et al. 2025). No correlation with DS was observed. The pre-factors A_1 and A_2 were found to increase linearly with concentration.

The chain conformation inside the correlation blob is expected to be rod-like because chains are strongly stretched by electrostatics, so that for $q \gtrsim 2\pi/\xi$, the scattering intensity should scale as $I(q) \sim q^{-1}$. This dependence is consistent with SANS data from previous studies for NaCMC in aqueous solution. The

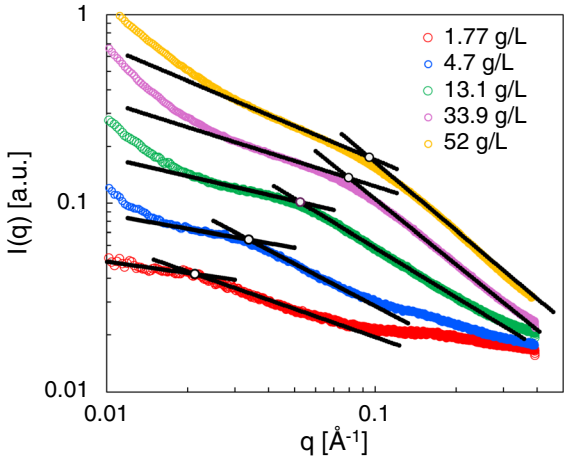

Fig. 4 Scattering profiles for S1 at different concentrations, indicated on the legend. Lines are fits to Eq. 5 and full circles indicate $(I(q^*), q^*)$ for each concentration. Data measured at SPring-8 synchrotron

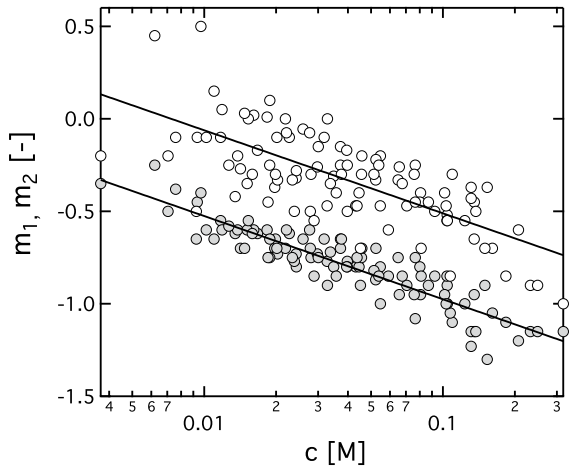

Fig. 5 Variation of m_1 (hollow symbols) and m_2 (full symbols) with concentration. Data include all samples studied. Lines are logarithmic lines to guide the eye

value of m_2 plotted in Fig. 5, which describes the power-law of the scattering intensity for $q \gtrsim 2\pi\xi^{-1}$ decreases with concentration over the entire range studied. For low concentrations, the weaker than -1 exponent may be explained as arising from the contribution of the q-independent background scattering term, which is apparent, for example in the red curve in Fig. 4. At high concentrations, m_2 takes values lower than -1. The interpretation of this exponent is not obvious to us: bending inside the correlation blob is unlikely because for $c \gtrsim 0.07$ M, the correlation length becomes smaller than the bare Kuhn length. A possibility is that even at high q the contribution of the intermolecular structure factor remains significant, so that m_2 does not reflect the behaviour of the form factor of the chains inside the correlation blob.

Correlation length and the stretching parameter

The position of the correlation peak measured by SANS and SAXS yield identical values for NaCMC, see Gulati et al. (2024). The correlation length was also shown to be independent of temperature (Lopez et al. 2015) and ion type for the alkali series (Gulati et al. 2024). The DS has a weak or null influence on the position of the correlation peak of NaCMC solutions, except at very high concentrations because for low DS samples, a fraction of the polymer aggregates and does not contribute to the mesh (Lopez et al. 2018; Barba et al. 2002; Kamide et al. 1985).

The peak or shoulder positions (q^*) can be used to calculate the correlation length according to:

$$\xi = \frac{2\pi}{q^*} \tag{6}$$

The correlation length for the various sodium and magnesium salts of CMC studied is plotted as a function of concentration in Fig. 6. Both salts display a scaling of $\xi \sim c^{-1/2}$, in agreement with the theoretical prediction of the Dobrynin model (Dobrynin et al. 1995). Note that for $c \gtrsim 0.035$ M for the sodium salt, the correlation length becomes smaller than the bare Kuhn length ($l_K \simeq 100$ Å, see Lopez 2020). For the magnesium salt, this cross-over occurs at $c \simeq 0.07$ M.

The scaling theory relates the correlation length to the stretching parameter B as (Dobrynin et al. 1995):

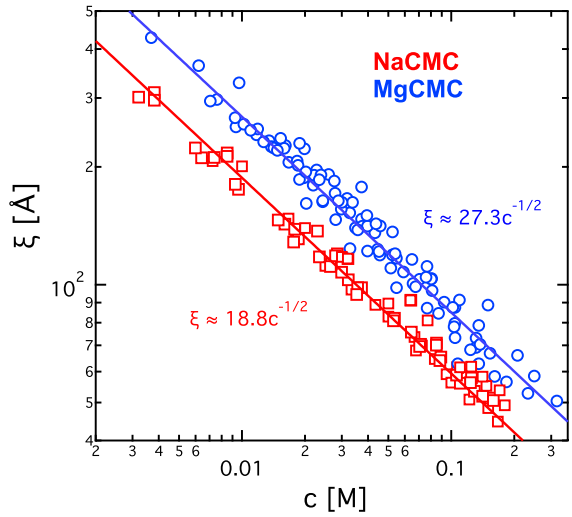

Fig. 6 Correlation length of sodium and magnesium salts of CMC in aqueous solution without added salts. Data for NaCMC are from Lopez et al. (2015, 2018), Hou et al. (2025); Sharratt et al. (2020) and Gulati et al. (2024) and this work. Data for MgCMC are from this work. Lines are best-fit power-laws with the exponent fixed to $-1/2$. Figure S2 plots the same data but with different symbols used for each polymer and literature study

$$\xi = \left(\frac{B}{bc}\right)^{1/2} \tag{7}$$

where b is the chemical monomer size, which is $\simeq 5$ Å for cellulose polymers and B is the stretching parameter, which describes the degree of chain coiling inside the correlation blob, with $B = 1$ corresponding to fully stretched chains and $B > 1$ to partial coiling.

The stretching parameter for NaCMC is found to be $B \simeq 1.1$ and for MgCMC $B \simeq 2.3$. This means that in dilute solution, NaCMC chains should have an end-to-end distance $\simeq 2.1\times$ larger than MgCMC. Based on this, we expect the overlap concentration of NaCMC to be $\simeq \times 2.1^3 \simeq 9$ lower than MgCMC, which contrasts with results from an earlier study (Lopez and Richtering 2019), where viscosimetric estimates for the overlap concentrations of the sodium and magnesium salts of sample S1 found a ratio of 3, implying that the stretching parameter for MgCMC is 1.4 times larger than for NaCMC.

The relatively large change in the stretching parameter with counterion valence contrasts with the independence of B on counterion type for monovalent counterions of the alkali series (Gulati et al. 2024).

Similar results have been reported for polystyrene sulfonate (PSS): the correlation lengths of various alkali metal salts of PSS as well as its acid form were found to be nearly identical by Kaji and co-workers (Kaji et al. 1984). By contrast, PSS with Mg^{2+} or Ca^{2+} counterions displays larger correlation lengths, corresponding to greater values of B (Lopez et al. 2021; Combet et al. 2005, 2011). This phenomenon likely arises because the charge density of a polyelectrolyte is strongly dependent on the counterion valence, but not on the counterion size, see below.

Local conformation

Following our earlier work, SANS data were fitted to the worm-like chain model in the high q region using the following equation (Lopez et al. 2015; Kassapidou et al. 1997):

$$I(q) = K\frac{\pi}{b'q}e^{-R_C^2q^2/4} + I_B \tag{8}$$

where K is a contrast factor, which is nearly identical for NaCMC and MgCMC due to the weak contrast between the counterions and the deuterated solvent background, b' is the z-projected monomer length, R_C is the chain's cross-sectional radius, which was set to 3.5 Å and I_B is a $q-$independent 'background' scattering intensity term. The procedure used here is presented in more detail in Lopez et al. (2015)

Eq. 8 applies only in the high-q region ($ql_K \gtrsim 1$), which is satisfied here given the relatively high persistence length 5 nm of the cellulose backbone, see Lopez (2020). The full worm-like chain form factor is more complex, see Pedersen and Gerstenberg (1996).

Equation 8 was found in earlier work to give reasonable values for b' of NaCMC, see Lopez et al. (2015, 2018). On the other hand, for MgPSS in aqueous solutions, we found that the extracted z-projected monomer length was similar to that of NaPSS, despite the more coiled concentration expected from the larger B parameter of MgPSS compared to NaPSS Lopez et al. (2021). Applying Eq. 8 to NaCMC and MgCMC samples at the same concentration suggests a higher value of b' for MgCMC than NaCMC. This is inconsistent with the measured B parameter and the fact that the NaCMC chain seems to be fully stretched inside the correlation blob. We do not have an explanation for this.

Low-q upturn

In the low-q region ($\lesssim 0.01$ Å^{-1}), the scattering intensity from the SAXS capillaries was too high to allow for reliable background subtraction. SANS measurements on the other hand allow for the low-q intensity to be measured with high accuracy. SANS curves for MgCMC in D_2O measured at the D11 beamline are shown in Fig. 7. For all concentrations, an upturn in the low-q region of the spectra is observed. The power-law of $\simeq -3$ is typical for mass fractals. This power-law exponent is weaker (less negative) than the value of $-$ 3.6 found for NaCMC in DI water in previous studies, which is characteristic of surface fractals (Lopez et al. 2015; Gulati et al. 2024). The curves measured at the NGB30m source display a slightly higher power-law which is in better agreement with the exponent observed for NaCMC in earlier studies, see the supporting information. The shape and intensity of the low-q upturn is known to depend on sample preparation, but it is unclear how this could lead to a change from a mass fractals to a surface fractals.

Conductivity

Aqueous solutions of NaCMC and MgCMC polymers with various degrees of substitution were prepared at concentrations around 0.1−0.15 M, as higher

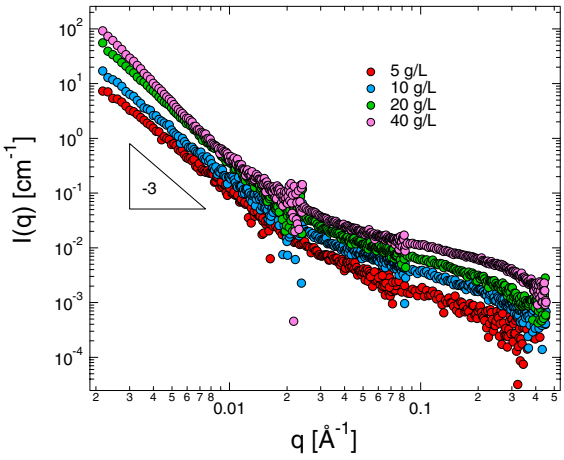

Fig. 7 Background subtracted SANS intensity MgCMC with different concentrations. Low-q upturn displays a power-law of $I(q) \propto q^{-3}$, indicated by the triangle. The sample cell was subtracted when reducing the data and an additional q-independent 'background' term (I_B) in Eq. 8 was subtracted for this plot

concentrations were too viscous for accurate conductivity measurement. Dilutions by a factor of $\simeq \times 1.5$ were then performed for each sample, and the conductivity of each sample was recorded at its respective concentration. This dilution process continued until the conductivity approached approximately 20 µS/cm. At this point, the conductivity is only $\simeq$ 7–10 higher than that of the solvent and estimates of the specific conductance become unreliable. All measurements were conducted at a controlled temperature of 25± 0.05 °C, with a water bath ensuring thermal stability. Thermogravimetric analysis (TGA) was used to quantify the residual moisture in CMC samples. TGA revealed that the average moisture contents in these samples were $\simeq$ 13% and 15% for NaCMC and MgCMC respectively and the values did not show any impact of the DS, see Fig. S2. The values of the water content were used to adjust the actual concentrations of CMC solutions.

Figure 8 shows the specific conductance ($\Lambda = \kappa/c$) of CMC polymers as a function of concentration with monovalent and divalent counterions. The CMC polymers have a DS ranging from 0.72 to 1.4. At lower concentrations, an upturn in the chemical conductivity is seen which can be due to the existence of residual salts in the solution. With increasing concentration, the specific conductance levels off at a constant value since the interference of the residual salt is less important.

As the DS in NaCMC increases (Fig 8a), we observe a corresponding increase in the electrical conductivity of NaCMC. Sample S3 with DS = 0.72 has the lowest chemical charge density of an ionic group per 7 Å ($u \simeq 1$), and S7 (DS = 1.4) has the highest chemical charge density of an ionic group per 3.5 Å ($u \simeq 2$). While the chemical charge density doubles from S3 to S7, the conductance does not increase proportionally. This is because condensed counterions neutralize some of the charged groups on the backbone, suppressing the overall charge density and electrical conductivity of the solution.

The model of Colby et al. (1997) gives the specific conductance of a salt-free polyelectrolyte solution as:

$$\Lambda = f\left[\lambda_C + fc\frac{N_A^2\xi^2e^2ln(\xi/D)}{3\pi\eta_s}\right] \tag{9}$$

where ξ is the correlation length, D is the cross-sectional diameter of the chain, η_s the viscosity of the solvent, c is the concentration in moles of monomers (glucose units) per volume, and f is the fraction of

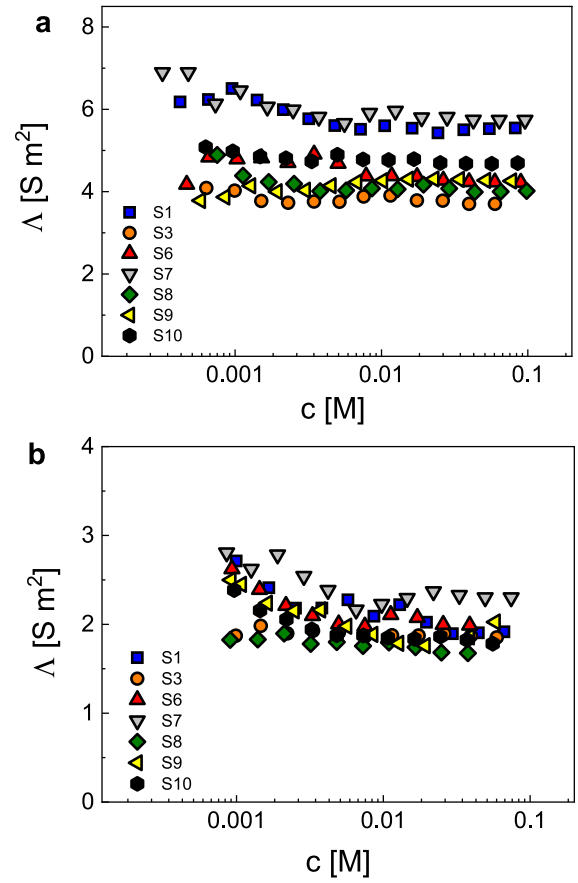

Fig. 8 Conductance of carboxymethyl cellulose with different DS as a function of concentration **a** with monovalent counterion (NaCMC) **b** with divalent counterion (MgCMC)

monomers with a dissociated counterion. The concentration of free counterions is fc/z. The maximum possible value of f is DS, corresponding to the case where all counterions are dissociated. λ_C is the equivalent conductance the counterion in units of Sm^2/mol, $\lambda_C = \lambda'_C/z$, where λ'_C is the molar conductance of the counterion and z the valence of the counterion, see Table 2. (Bordi et al. 2004) give an additional factor of z in the second term inside the square brackets of Eq. 9, which should not be there.

Equation 9 is a quadratic equation in f. Knowing the values of ξ, D and the various constants, f can be calculated for any concentration from the measured value of Λ.

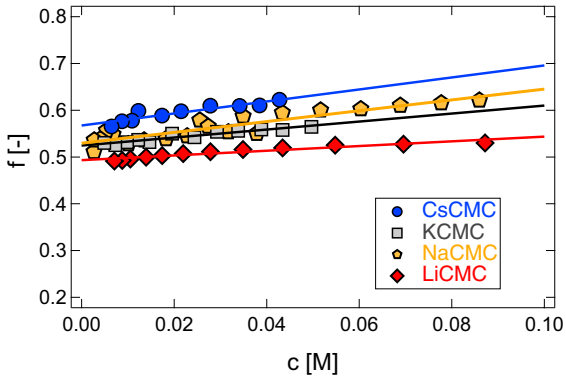

Fig. 9 Fraction of monomers bearing a dissociated counterion as a function of concentration for different alkali metal salts of S2. Lines are guides to the eye. Data for NaCMC combine results from this work and Hou et al. (2024a)

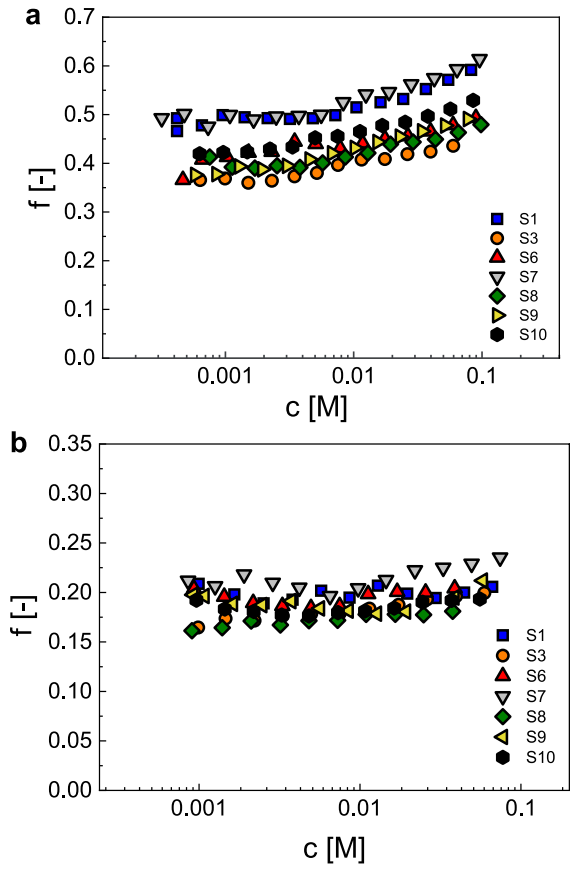

Fig. 10 **a** Fraction of monomers with a dissociated counterion for NaCMC with different DS values as a function of polymer concentration **b** same as part a but for MgCMC solutions. Values of f are calculated with Eq. 9 and the ξ data from Fig. 6

Influence of counterion type

Figure 9 plots the fraction of monomers with a dissociated counterion for sample S2 (DS $\simeq 0.9$) with different alkali metal counterions. All four salts show a slow increase in the fraction of ionised monomers with concentration. The value of f depends weakly on the counterion type, with the difference between LiCMC and CsCMC being $\simeq 20\%$. The order of counterion dissociation observed for the alkali metal counterions is qualitatively consistent with the model of Oosawa, which expects that larger counterions dissociate to a greater extent and also with that of Ghosh and Kundagrami (2024). Our results are also in line with studies by various groups using electrical conductivity (Trivedi and Patel 1986; Milas 1969, 1974) and osmotic pressure (Milas 1974)

Despite the large differences in site-binding strength for the alkali metal counterions which are apparent from the ultrasound absorption measurements by Milas and co-worker (Milas 1974; Zana et al. 1971) (Fig. 2a), their influence in counterion condensation are minimal. This suggests that site-binding for the CMC-alkaline metal system does not induce counterion condensation. Instead, site-bound counterions are a sub-set of condensed counterions. Some evidence against this view can be found in the activity coefficient of K^+ counterions in Dextran sulfate (Satake et al. 1972; Noguchi et al. 1973). This may be a peculiarity of branched polyelectrolytes or it may reflect the stronger site-binding strength of alkali ions to Dextran derivatives.

Influence of DS and counterion valence on the fraction of free counterions

Figure 10 shows the fraction of monomers with a dissociated counterion as a function of concentration across different degrees of substitution. The correlation length at each polymer concentration is calculated from the data in Fig. 6: $\xi = 18.8c^{-1/2}$ for NaCMC, and $\xi = 27.3c^{-1/2}$ for MgCMC, independent of DS. By incorporating the correlation length

and the conductivity at each concentration into Eq. 9, the fraction of monomers bearing a dissociated counterion is calculated. We choose a value of $D = 7$ Å for the cross-sectional diameter of chains, independent of DS (Lopez et al. 2015, 2018). For all degrees of substitution, the fraction of free counterions follows an approximately linear relationship with concentration, see also Fig. 9.

According to OM condensation theory, polyelectrolytes with high charge densities, in dilute solutions, have an effective charge density of $\mu_{eff} = e/l_B$, i.e. one charge per Bjerrum length along the chain contour. With this assumption, OM predicts that fraction of monomers bearing a dissociated counterion is $f = b_c/(z_C l_B)$ where b_c is the distance between ionic groups along the backbone, which can be considered either as the monomer length ($b \simeq 5.15$ Å), or the monomer length divided by the stretching parameter (b/B). For NaCMC, the stretching parameter obtained by SAXS and SANS analysis is $\simeq 1.1$, independent of DS (Lopez et al. 2018). The OM threshold corresponds to DS $\simeq 0.6$–0.7 for NaCMC in water.

At concentrations below 0.01 M, an approximately constant value for f is observed, varying from 0.34 for DS = 0.72 to 0.5 for DS = 1.4. The counterion fraction at DS = 1.4 is close to OM predictions (0.6) but deviates further away as the DS decreases. At the lowest degree of substitution, DS $\simeq 0.7$, the OM theory expects no counterion condensation (i.e. $f \simeq$ DS) but the measured value of f approximately half of this value. The discrepancy may arise, at least in part, due to the heterogeneity of substitution of the polymer: for a homogeneously substituted sample with DS $\simeq 0.7$, the spacing between each charge is equal to the Bjerrum length and no condensation is expected. If substitution heterogeneous, regions of high substitution co-exist with less substituted ones. In the more substituted regions, the charge spacing will be smaller than l_B leading to condensation. This provides a plausible explanation for why condensation is observed in heterogeneous systems even when the *average* charge spacing is larger than the l_B. The average value of f, for divalent MgCMC, is calculated to be $f \simeq 0.2$, $\times \simeq 2$ lower than the value for NaCMC, in agreement with OM theory.

Figure 11 compares how the DS influences the fraction of monomers with a free counterion in Na and MgCMC. In both cases, a linear dependence of f on the DS is observed, with the slope for the sodium

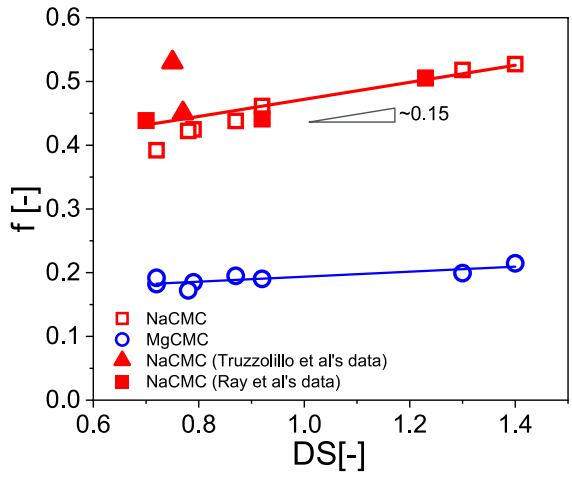

Fig. 11 Fraction of monomers bearing a dissociated counterion as a function of DS. Hollow symbols are from this work and full symbols evaluate f from the conductivity data of Ray et al extrapolated to $T = 25$ °C using the same method as for our samples. Estimates for f by Truzzzolillo et al, based on solution conductivity but employing a different method to calculate f are also included for comparison. Red symbols are for NaCMC and blue symbols for MgCMC

salts being larger than for MgCMC. The weak influence of DS on the fraction of charged monomers contrasts with the large influence DS has on chain dynamics observed for NaCMC solutions: for DS $\lesssim 0.9$, associative interactions between chains become important at high concentrations ($c \gtrsim 0.05$ M), leading to physical gelation (Elliot and Ganz 1974; Lopez et al. 2018; Lopez and Richtering 2021). Such associations appear to have no clear influence on the fraction of dissociated counterions or the polyion conductivity. Rheology data for weakly substituted MgCMC solutions are not available.

The conductivity data of Ray et al. (2016) for solutions of NaCMC in DI water were extrapolated to $T = 25$ °C and used to evaluate f by the same procedure as for our data. The results are in good agreement with our data. Truzzolillo et al estimate the charge fraction of NaCMC based on conductivity data but using a different procedure to the one employed here. Their results for two NaCMC polymers are plotted in Fig. 11 as red triangles. One of their samples agrees well with our results while the other displays a value of $f \simeq 20\%$ higher than the other estimates (Table 3).

Table 3 Comparison of estimates for the fraction of charged monomers for CMC with DS ≃ 1.2−1.3 according to different methods

Method	DS ≃ 1.3		DS ≃ 0.8		Refs.
	f_{Na}	f_{Mg}	f_{Na}	f_{Mg}	
Conductivity	0.5	0.22	0.45	0.2	This work (Ray et al. 2016)
Ion selective potentiometry[c]	0.72	0.3	0.58	–	Rinaudo et al. (1973), Rinaudo and Milas (1971, 1974, 1975, 1978), Rinaudo (1973), Nagasawa and Kagawa (1957), see Fig. 1
Vapour pressure osmometry	0.67[d]	–	–	–	Rinaudo et al. (1973), Rinaudo and Milas (1975)
Membrane osmometry	0.69[d]	0.37[e]	–	–	Rinaudo et al. (1973), Rinaudo and Milas (1975)
Dielectric spectroscopy[a]	–	–	0.3	–	Truzzolillo et al. (2009)
Viscosity[b]	0.42	–	–	–	Lopez et al. (2017) and Matsumoto et al. (2025)
Viscosity[a]	0.15	0.09	–	–	Jacobs et al. (2021)

[a]Based on applying Dobrynin's quantitative scaling to salt-free viscosity data

[b]Based on applying Dobrynin et al's 1995 scaling model to the decrease of solution viscosity with added salt

[c] Values are interpolated to DS = 1.3 from data in Fig. 1. Estimates of f are using Oosawa's model which equates counterion activity with f

[d] interpolated from data in the DS = 1.1–2.5 range

[e] Approximated from Rinaudo et al's result for CaCMC with DS = 1.6, assuming the charge fraction is the same as DS = 1.3. Osmometry estimates for f are obtained assuming each dissociated counterion contributes k_BT to the osmotic pressure and condensed counterions are osmotically inactive

Comparison of methods to estimate counterion condensation

The conductivity data from this study and others yield consistent results for the fraction of charged monomers of NaCMC. Next, we try to establish wether different methods of estimating the fraction of free counterions also yield consistent results. We assume that the counterion activity and the osmotic coefficient of the counterions is equal to the fraction of free counterions. This corresponds to the Oosawa theory (Oosawa 1971). These values are somewhat larger than those obtained from the conductivity data for sodium and magnesium salts of CMC with DS = 1.3 and 0.8. A possible explanation is as follows: the model of Colby et al assumes that free (non-condensed) counterions have the same mobility as in a solution of a simple salt, but experimental measurements, in agreement with theoretical predictions show that free polyelectrolyte counterions have a diffusion coefficient ≃ 30% lower than that of the ion in simple salt solutions (Ander and Kardan 1984). If the mobility in Eq. 9 is adjusted by a similar pre-factor, the conductivity estimates for f_{Na} and f_{Mg} increase by ≃ 10–15%, bringing them closer to the potentiometry and osmometry estimates. Given the limited osmotic pressure data, experimental error should not be ruled out as a possible cause of the disagreement.

Bordi et al. used the following equation to evaluate the fraction of charged monomers from dielectric spectroscopy data (Bordi et al. 2004):

$$f = \frac{\Delta\epsilon}{6\pi\omega_C D_{CI} l_B \epsilon c} \tag{10}$$

here $\Delta\epsilon$ is the dielectric increment and ω_C the characteristic frequency of the intermediate relaxation decay, see Bordi et al. (2004). D_{CI} is the diffusion coefficient of the counterion (1.3×10^{-9} m^2/s).

Using the dielectric spectroscopy data of Truzzolillo et al. (2009), we estimate $f \simeq 0.3$ for their two samples with DS ≃ 0.8. The value from Eq. 10 is lower than the conductivity and potentiometric estimates for NaCMC with this DS. This contrasts with the NaPSS system, where Bordi et al showed that Eq. 10 gives f values which are ≃ × 5 higher than those from conductivity and osmotic pressure data.

The fraction of charged monomers obtained from the decrease in the viscosity of NaCMC solutions upon salt addition obtained by Matsumoto et al. (2025) agrees reasonably well with our conductivity

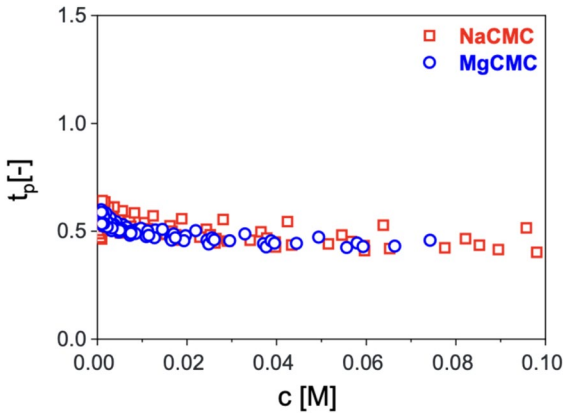

Fig. 12 Transference number of the polyion (t_p) in aqueous carboxymethylcellulose solutions with a mono (NaCMC) and divalent (MgCMC) counterions as a function of the polyelectrolyte concentration

estimate. By contrast the viscosimetric estimate from Dobrynin's quantitative scaling appears too low (Jacobs et al. 2021).

In summary, the various methods considered yield results which agree qualitatively. Due to the limited data available for all methods other than conductivity, it is not possible, at present, to draw any solid conclusions on the reasons for the lack of quantitative agreement.

Transference number

The transference number of the polyion (t_p) is calculated as the ratio of the second term inside the square brackets in Eq. 9 to the sum of both terms inside the square brackets.

Figure 12 shows the transference number of the polyion plotted against the equivalent concentration of the polyelectrolyte for all samples. The transference number of NaCMC and MgCMC are found to be close to 0.5 and independent of ion valence. This result is consistent with Ray et al's data for NaCMC which shows t_p is nearly independent of charge density. Note that their polyion transference number is equivalent to t_p/f in this work. (Gulati et al. 2026) found that the transference number of the tetrabutylammonium salt of CMC increases weakly with the effective charge of the chain and Diederichsen et al. (2019) reported approximately equal t_P values for short polysulfone derivatives in water and DMSO, though the effective charge fraction is expected to be higher in water owing to the higher dielectric constant.

Conclusions

This study examined the effects of counterion type and charge density on the structural and electrostatic properties of carboxymethyl cellulose (CMC) in aqueous solutions. Small-angle X-ray and neutron scattering (SAXS/SANS) reveal structural differences between NaCMC and MgCMC. MgCMC solutions lacked the well-defined correlation peaks seen for NaCMC, instead displaying broad scattering shoulders, which suggests a less ordered local structure due to weaker electrostatic repulsion. While NaCMC chains remained locally extended with a stretching parameter $B \simeq 1.1$, MgCMC exhibited significant coiling ($B \simeq 2.3$).

The fraction of charged monomers f was consistently higher for NaCMC (0.4–0.5) than for MgCMC (0.19–0.21), in quantitative agreement with the OM theory, which expects the charge fraction to vary inversely with the counterion valence. The experimental values of f fall below theoretical predictions, particularly for low-DS samples, perhaps due to the heterogeneous distribution of charged groups along the CMC backbone. While monovalent alkali counterions (Li^+ to Cs^+) show only minor variations in f, despite differences in site-binding affinity, the switch from Na^+ to Mg^{2+} resulted in a sharp decline in charge dissociation, highlighting the dominant role of valence over ion-specific effects in condensation.

Acknowledgements We are grateful to the SPring-8 synchrotron and NIST center for neutron research for beamtime (no. 26007) and Susan Krueger for help with the experiments and data reduction. We thank Dr. Noboru Ohta for his assistance at SPring-8 beamline BL40B2, in support of the experiments under proposal number 2024A1203. We would also like to thank Bahar Baniasadi (PSU), Prof. Atsushi Matsumoto (University of Fukui), Himari Taniguchi, Marina Ikeda, Yume Tao, Rene Iwato, Hikari Tsunekawa, Hinako Nakayama, Kyoka Hinomoto, Taiki Okamoto, Naruki Kanda (Okayama University), Anish Gulati and Hannes Luhmann (RWTH) for their contribution in sample preparation and measurements at BL40B2. We are grateful for Dow and CP Kelco for donating NaCMC polymers. We thank Will Sharratt (University of Liverpool) and Joao Cabral (Imperial College London)

for measuring SANS samples at the D11 beamline. We thank Andrey Dobrynin (UNC Chapel Hill) for useful discussions and for providing feedback on a draft of the manuscript. This work was partially supported by JSPS KAKENHI Grant Number JP24K01236 and JP20KK0325. F.H. acknowledges the support of the Intramural Research Program of the Eunice Kennedy Shriver National Institute of Child Health and Human Development, National Institutes of Health. CGL acknowledges funding from the DFG, project number GO 3250/2-1.

Author contributions E.A.: Experimental measurements, data analysis, writing, editing T.W.: Experiments, funding, beamtime proposal writing, writing, editing. F.H.: Experiments, proposal writing, data interpretation C.H.: Experiments, beamtime proposal writing, writing, editing. C.G.L: Experiments, beamtime proposal writing, funding, data analysis and interpretation, writing, editing M.H.: Experiments, beamtime proposal writing, data analysis and interpretation, writing, editing.

Funding Open Access funding enabled and organized by Projekt DEAL. This work was supported by DFG (grant number GO 3250/2-1) and JSPS KAKENHI (Grant numbers JP24K01236 and JP20KK0325).

Data availability All research data (Conductivity, scattering and TGA) are provided in the supplementary information files.

Declarations

Conflict of interest The authors have no relevant financial or non-financial interests to disclose.

Open Access This article is licensed under a Creative Commons Attribution 4.0 International License, which permits use, sharing, adaptation, distribution and reproduction in any medium or format, as long as you give appropriate credit to the original author(s) and the source, provide a link to the Creative Commons licence, and indicate if changes were made. The images or other third party material in this article are included in the article's Creative Commons licence, unless indicated otherwise in a credit line to the material. If material is not included in the article's Creative Commons licence and your intended use is not permitted by statutory regulation or exceeds the permitted use, you will need to obtain permission directly from the copyright holder. To view a copy of this licence, visit http://creativecommons.org/licenses/by/4.0/.

References

Adamson A (1979) A textbook of physical chemistry. Elsevier, Amsterdam

Agrawal A, Radakovic A, Vonteddu A, Rizvi S, Huynh VN, Douglas JF, Tirrell MV, Karim A, Szostak JW (2024) Did the exposure of coacervate droplets to rain make them the first stable protocells? Sci Adv 10(34):eadn9657

Ander P, Kardan M (1984) Interactions of sodium ions with polyelectrolytes of varying charge density. Macromolecules 17(11):2431–2436

Arumughan V, Ozeren HD, Hedenqvist M, Skepo M, Nypelo T, Hasani M, Larsson A (2023) Anion-specific adsorption of carboxymethyl cellulose on cellulose. Langmuir 39(42):15014–15021

Barba C, Montané D, Rinaudo M, Farriol X (2002) Synthesis and characterization of carboxymethylcelluloses (CMC) from non-wood fibers I. Accessibility of cellulose fibers and CMC synthesis. Cellulose 9:319–326

Behra JS, Mattsson J, Cayre OJ, Robles ES, Tang H, Hunter TN (2019) Characterization of sodium carboxymethyl cellulose aqueous solutions to support complex product formulation: a rheology and light scattering study. ACS Appl Polym Mater 1(3):344–358

Beyer D, Holm C (2024) Unexpected two-stage swelling of weak polyelectrolyte brushes with divalent counterions. ACS Macro Lett 13(9):1185–1191

Bordi F, Cametti C, Colby R (2004) Dielectric spectroscopy and conductivity of polyelectrolyte solutions. J Phys Condens Matter 16(49):R1423

Cai Y, Li D, Peng S, Liu H (2025) Synthesis of dual-responsive carboxymethyl cellulose-based nanogels for drug delivery applications. Colloid Polym Sci 303(2):287–300

Chang R, Yethiraj A (2003) Brownian dynamics simulations of polyelectrolyte solutions with divalent counterions. J Chem Phys 118(24):11315–11325

Chen G, Perazzo A, Stone HA (2021) Electrostatics, conformation, and rheology of unentangled semidilute polyelectrolyte solutions. J Rheol 65(4):507–526

Chremos A, Douglas JF (2016) Influence of higher valent ions on flexible polyelectrolyte stiffness and counter-ion distribution. J Chem Phys 144(16):164904

Chremos A, Douglas JF (2017) Communication: counter-ion solvation and anomalous low-angle scattering in salt-free polyelectrolyte solutions. J Chem Phys 147(24):241103

Chremos A, Douglas JF (2018) Polyelectrolyte association and solvation. J Chem Phys 149(16):163305

Colby RH (2010) Structure and linear viscoelasticity of flexible polymer solutions: comparison of polyelectrolyte and neutral polymer solutions. Rheol Acta 49:425–442

Colby RH, Boris DC, Krause WE, Tan JS (1997) Polyelectrolyte conductivity. J Polym Sci Part B Polym Phys 35(17):2951–2960

Collins KD (2004) Ions from the Hofmeister series and osmolytes: effects on proteins in solution and in the crystallization process. Methods 34(3):300–311

Combet J, Isel F, Rawiso M, Boué F (2005) Scattering functions of flexible polyelectrolytes in the presence of mixed valence counterions: condensation and scaling. Macromolecules 38(17):7456–7469

Combet J, Rawiso M, Rochas C, Hoffmann S, Boué F (2011) Structure of polyelectrolytes with mixed monovalent and divalent counterions: Saxs measurements and Poisson–Boltzmann analysis. Macromolecules 44(8):3039–3052

Danielsen SP, Panyukov S, Rubinstein M (2020) Ion pairing and the structure of gel coacervates. Macromolecules 53(21):9420–9442

Diederichsen KM, Terrell RC, McCloskey BD (2019) Counterion transport and transference number in aqueous and nonaqueous short-chain polyelectrolyte solutions. J Phys Chem B 123(50):10858–10867

Dobrynin AV, Colby RH, Rubinstein M (1995) Scaling theory of polyelectrolyte solutions. Macromolecules 28(6):1859–1871

Dobrynin AV, Rubinstein M (2005) Theory of polyelectrolytes in solutions and at surfaces. Prog Polym Sci 30(11):1049–1118

Dubois E, Boué F (2001) Conformation of poly (styrenesulfonate) polyions in the presence of multivalent ions: small-angle neutron scattering experiments. Macromolecules 34(11):3684–3697

Ehtiati K, Moghaddam SZ, Klok H-A, Daugaard AE, Thormann E (2022) Specific counterion effects on the swelling behavior of strong polyelectrolyte brushes. Macromolecules 55(12):5123–5130

Elliot JH, Ganz A (1974) Some rheological properties of sodium carboxymethylcellulose solutions and gels. Rheol Acta 13(4):670–674

Ermi BD, Amis EJ (1998) Domain structures in low ionic strength polyelectrolyte solutions. Macromolecules 31(21):7378–7384

Essafi W, Lafuma F, Williams C (1999) Structural evidence of charge renormalization in semi-dilute solutions of highly charged polyelectrolytes. Eur Phys J B Condens Matter Complex Syst 9:261–266

Ghosh S, Kundagrami A (2024) Effect of counterion size on polyelectrolyte conformations and thermodynamics. J Chem Phys 160(8):084909

Glisman A, Mantha S, Yu D, Wasserman EP, Backer S, Wang Z-G (2024) Multivalent ion-mediated polyelectrolyte association and structure. Macromolecules 57(5):1941–1949

Gregory KP, Elliott GR, Robertson H, Kumar A, Wanless EJ, Webber GB, Craig VS, Andersson GG, Page AJ (2022) Understanding specific ion effects and the Hofmeister series. Phys Chem Chem Phys 24(21):12682–12718

Gulati A, Douglas JF, Matsarskaia O, Lopez CG (2024) Influence of counterion type on the scattering of a semiflexible polyelectrolyte. Soft Matter 20(43):8610–8620

Gulati A, Meng L, Hou C, Watanabe T, Lopez C (2026) Solution structure and counterion condensation of carboxymethyl cellulose in organic solvents. Submitted to ACS Applied Polymer Materials

Hedlund A, Germgård U (2007) Some aspects on the kinetics of etherification in the preparation of CMC. Cellulose 14:161–169

Hemmes P (1972) Volume changes of ionic association reactions. J Phys Chem 76(6):895–900

Hen J, Strauss UP (1974) Counterion binding by poly (vinyl sulfonate). J Phys Chem 78(10):1013–1017

Horkay F, Douglas JF (2025) Effect of divalent ions on the structure of polyelectrolyte gels. Polymer 327:128311

Horkay F, Hammouda B (2008) Small-angle neutron scattering from typical synthetic and biopolymer solutions. Colloid Polym Sci 286:611–620

Hotton C, Ducouret G, Sirieix-Plénet J, Bizien T, Porcar L, Malikova N (2023) Tuning structure and rheological properties of polyelectrolyte-based hydrogels through counterion-specific effects. Macromolecules 56(3):923–933

Hotton C, Sakhawoth Y, Rollet A-L, Sirieix-Plénet J, Tea L, Combet S, Sharp M, Hoffmann I, Nallet F, Malikova N (2024) Ion-specific effects in polyelectrolyte solutions: chain–chain interactions, chain rigidity and dynamics. C R Chim 27(S5):1–13

Hou C, Watanabe T, Lopez CG, Richtering W (2025a) Structure and rheology of carboxymethylcellulose in polar solvent mixtures. Carbohydr Polym 347:122287

Hou J, Chang H, Liu Y, Zhang H, Li H, Wang Z, Rayan AM, Ghamry M, Mohamed TA, Zhao K (2024b) Exploring the phase behavior of natural egg yolk–carboxymethyl cellulose concentrate: impact on emulsification and gelling properties. Food Hydrocolloids 157:110385

Hou C, Richtering W, Watanabe T, Leonhard K, Papusha M, Lopez CG (2025b) Solutions of carboxymethylcellulose with organic counterions (I): the influence of counterion properties on the polymer structure and solubility. Macromolecules 58(14):7489–7499

Jacobs M, Lopez CG, Dobrynin AV (2021) Quantifying the effect of multivalent ions in polyelectrolyte solutions. Macromolecules 54(20):9577–9586

Jimenez LN, Martínez Narváez CD, Sharma V (2020) Capillary breakup and extensional rheology response of food thickener cellulose gum (NACMC) in salt-free and excess salt solutions. Phys Fluids 32(1):012113

Jimenez LN, Martinez Narvaez CD, Sharma V (2022) Solvent properties influence the rheology and pinching dynamics of polyelectrolyte solutions: thickening the pot with glycerol and cellulose gum. Macromolecules 55(18):8117–8132

Kaji K, Urakawa H, Kanaya T, Kitamaru R (1984) Distance distribution analysis of small-angle x-ray scattering for semidilute polyelectrolyte solutions without salts. Macromolecules 17(9):1835–1839

Kamide K, Okajima K, Kowsaka K, Matsui T, Nomura S, Hikichi K (1985) Effect of the distribution of substitution of the sodium salt of carboxymethylcellulose on its absorbency toward aqueous liquid. Polym J 17(8):909–918

Kassapidou K, Jesse W, Kuil M, Lapp A, Egelhaaf S, Van der Maarel J (1997) Structure and charge distribution in DNA and poly (styrenesulfonate) aqueous solutions. Macromolecules 30(9):2671–2684

Kherb J, Flores SC, Cremer PS (2012) Role of carboxylate side chains in the cation Hofmeister series. J Phys Chem B 116(25):7389–7397

Kim Y, Kim S, Kim BS, Park JH, Ahn KH, Park JD (2022) Yielding behavior of concentrated lithium-ion battery anode slurry. Phys Fluids 34(12):123112

Koda S, Sugi Y, Sakurai T, Matsuoka T, Nomura H (2004) Study on segmental motion and ion binding in polyelectrolyte solutions by ultrasonic spectroscopy. J Solution Chem 33:747–760

Komiyama J, Takeda Y, Ando M, Iijima T (1974) Dilatometric study of monovalent counter-ion association with polymethacrylate. Polymer 15(7):468–470

Komiyama J, Ando M, Takeda Y, Iuma T (1976) Dilatometric study of monovalent counter-ion association with carboxylates. Eur Polym J 12(3):201–207

Kondou S, Sakashita Y, Morinaga A, Katayama Y, Dokko K, Watanabe M, Ueno K (2023) Concentrated nonaqueous polyelectrolyte solutions: high Na-ion transference number and surface-tethered polyanion layer for sodium-metal batteries. ACS Appl Mater Interfaces 15(9):11741–11755

Kong P, Rosnan SM, Enomae T (2024) Carboxymethyl cellulose-chitosan edible films for food packaging: a review of recent advances. Carbohydr Polym 346:122612

Kono H, Oshima K, Hashimoto H, Shimizu Y, Tajima K (2016a) NMR characterization of sodium carboxymethyl cellulose 2: chemical shift assignment and conformation analysis of substituent groups. Carbohydr Polym 150:241–249

Kono H, Oshima K, Hashimoto H, Shimizu Y, Tajima K (2016b) NMR characterization of sodium carboxymethyl cellulose: substituent distribution and mole fraction of monomers in the polymer chains. Carbohydr Polym 146:1–9

Legrand G, Baeza GP, Peyla M, Porcar L, Fernández-de Alba C, Manneville S, Divoux T (2024) Acid-induced gelation of carboxymethylcellulose solutions. ACS Macro Lett 13(2):234–239

Liao Q, Dobrynin AV, Rubinstein M (2003) Molecular dynamics simulations of polyelectrolyte solutions: osmotic coefficient and counterion condensation. Macromolecules 36(9):3399–3410

Liu Y, Zhao K (2019) Rheological and dielectric behavior of milk/sodium carboxymethylcellulose mixtures at various temperatures. J Mol Liq 290:111175

Lopez CG (2020) Entanglement of semiflexible polyelectrolytes: crossover concentrations and entanglement density of sodium carboxymethyl cellulose. J Rheol 64(1):191–204

Lopez CG, Richtering W (2019) Influence of divalent counterions on the solution rheology and supramolecular aggregation of carboxymethyl cellulose. Cellulose 26:1517–1534

Lopez CG, Richtering W (2021) Oscillatory rheology of carboxymethyl cellulose gels: influence of concentration and pH. Carbohydr Polym 267:118117

Lopez CG, Rogers SE, Colby RH, Graham P, Cabral JT (2015) Structure of sodium carboxymethyl cellulose aqueous solutions: a sans and rheology study. J Polym Sci Part B Polym Phys 53(7):492–501

Lopez CG, Colby RH, Graham P, Cabral JT (2017) Viscosity and scaling of semiflexible polyelectrolyte NaCMC in aqueous salt solutions. Macromolecules 50(1):332–338

Lopez CG, Colby RH, Cabral JT (2018) Electrostatic and hydrophobic interactions in NaCMC aqueous solutions: effect of degree of substitution. Macromolecules 51(8):3165–3175

Lopez CG, Horkay F, Schweins R, Richtering W (2021) Solution properties of polyelectrolytes with divalent counterions. Macromolecules 54(22):10583–10593

Lopez CG, Matsumoto A, Shen AQ (2024) Dilute polyelectrolyte solutions: recent progress and open questions. Soft Matter 20(12):2635–2687

Lytle TK, Muralidharan A, Yethiraj A (2021) Why lithium ions stick to some anions and not others. J Phys Chem B 125(17):4447–4455

Manning GS (1969) Limiting laws and counterion condensation in polyelectrolyte solutions I. Colligative properties. J Chem Phys 51(3):924–933

Manning GS (1974) Limiting laws for equilibrium and transport properties of polyelectrolyte solutions. In Polyelectrolytes: papers initiated by a NATO Advanced Study Institute on Charged and Reactive Polymers held in France, June 1972. Springer, pp 9–37

Marcus Y, Hefter G (2006) Ion pairing. Chem Rev 106(11):4585–4621

Marioni N, Rajesh A, Zhang Z, Freeman BD, Ganesan V (2024) What is the influence of ion aggregation and counterion condensation on salt transport in ion exchange membranes? J Membr Sci 701:122713

Matsumoto A, Ukai R, Osada H, Sugihara S, Maeda Y (2022) Tuning the solution viscosity of ionic-liquid-based polyelectrolytes with solvent dielectric constants via the counterion condensation. Macromolecules 55(23):10600–10606

Matsumoto A, Ikeda M, Sugihara S, Maeda Y (2025) Viscometric method for estimating the charge fraction of polyelectrolytes in solutions. Nihon Reoroji Gakkaishi 53(1):1–10

Milas M (1969) Fixation sélective des cations sur un polyélectrolyte anionique. PhD thesis, Université de Grenoble

Milas M (1974) Intéraction avec les cations compensateurs et sélectivité ionique dans les solutions aqueuses de polyélectrolyte: influence de la densité de charge. PhD thesis, Université Scientifique et Médicale de Grenoble

Mussel M, Basser PJ, Horkay F (2019) Effects of mono- and divalent cations on the structure and thermodynamic properties of polyelectrolyte gels. Soft Matter 15(20):4153–4161

Muthukumar M (2004) Theory of counter-ion condensation on flexible polyelectrolytes: adsorption mechanism. J Chem Phys 120(19):9343–9350

Nagasawa M, Kagawa I (1957) Colligative properties of polyelectrolyte solutions. IV. Activity coefficient of sodium ion. J Polym Sci 25(108):61–76

Nishida K, Kaji K, Kanaya T (1995) Charge density dependence of correlation length due to electrostatic repulsion in polyelectrolyte solutions. Macromolecules 28(7):2472–2475

Nishida K, Kaji K, Kanaya T, Shibano T (2002) Added salt effect on the intermolecular correlation in flexible polyelectrolyte solutions: small-angle scattering study. Macromolecules 35(10):4084–4089

Noguchi H, Gekko K, Makino S (1973) Interaction of sodium and potassium ions with ionic dextran derivatives in aqueous solution with and without added salt. Macromolecules 6(3):438–442

Nova L, Stepanek M, Morozova I, Tosner Z, Uhlik F (2025) Ionization and chain size of weak polyelectrolytes in semidilute regime. Macromolecules 58(18):9962–9971

Oosawa F (1957) A simple theory of thermodynamic properties of polyelectrolyte solutions. J Polym Sci 23(103):421–430

Oosawa F (1971) Polyelectrolytes. Dekker

O'Shaughnessy B, Yang Q (2005) Manning–Oosawa counterion condensation. Phys Rev Lett 94(4):048302

Pedersen JS, Gerstenberg MC (1996) Scattering form factor of block copolymer micelles. Macromolecules 29(4):1363–1365

Pineda SP, Stano R, Murmiliuk A, Blanco PM, Montes P, Tosner Z, Groborz O, Panek J, Hruby M, Stepanek M et al (2024) Charge regulation triggers condensation of short oligopeptides to polyelectrolytes. JACS Au 4(5):1775–1785

Prabhu V, Muthukumar M, Wignall GD, Melnichenko YB (2003) Polyelectrolyte chain dimensions and concentration fluctuations near phase boundaries. J Chem Phys 119(7):4085–4098

Ray D, De R, Das B (2016) Thermodynamic, transport and frictional properties in semidilute aqueous sodium carboxymethylcellulose solution. J Chem Thermodyn 101:227–235

Rinaudo M (1973) Polyelektrolyteigenschaften von carboxymethylcellulose in wäßriger lösung-einfluß der ladungsdichte. Faserforsch Textiltech 4:21–28

Rinaudo MBL, Milas M (1971) Determination of dissociation constant of polyacids by potentiometry. C R Hebdomadaires Seances Acad Sci Ser C 273(18):1148

Rinaudo M, Milas M (1974) Interaction of monovalent and divalent counterions with some carboxylic polysaccharides. J Polym Sci Polym Chem Ed 12(9):2073–2081

Rinaudo M, Milas M (1975) Ionic selectivity of polyelectrolytes in salt free solutions. In: Polyelectrolytes and their applications. Springer, pp 31–49

Rinaudo M, Mils M (1978) Polyelectroyte behavior of a bacterial polysaccharide from xanthomonas campestris: comparison with carboxymethylcellulose. Biopolym Origin Res Biomol 17(11):2663–2678

Rinaudo M, Mazet J, Milas M (1973) Propriétés thermodynamiques des polyanions à densité de charge variable. C R Acad Sci pp 1401–1404

Robinson RA Stokes RH (2002) Electrolyte solutions. Courier Corporation

Różańska S, Verbeke K, Różański J, Clasen C, Wagner P (2019) Capillary breakup extensional rheometry of sodium carboxymethylcellulose solutions in water and propylene glycol/water mixtures. J Polym Sci Part B Polym Phys 57(22):1537–1547

Salamon K, Aumiler D, Pabst G, Vuletic T (2013) Probing the mesh formed by the semirigid polyelectrolytes. Macromolecules 46(3):1107–1118

Satake I, Fukuda M, Ohta T, Nakamura K, Fujita N, Yamauchi A, Kimizuka H (1972) Interactions of counterions with dextran sulfate in aqueous solutions. J Polym Sci Polym Phys Ed 10(12):2343–2354

Sharratt WN, O'Connell R, Rogers SE, Lopez CG, Cabral JT (2020) Conformation and phase behavior of sodium carboxymethyl cellulose in the presence of mono-and divalent salts. Macromolecules 53(4):1451–1463

Sharratt WN, Lopez CG, Sarkis M, Tyagi G, O'Connell R, Rogers SE, Cabral JT (2021) Ionotropic gelation fronts in sodium carboxymethyl cellulose for hydrogel particle formation. Gels 7(2):44

Sing CE, Qin J (2023) Bridging field theory and ion pairing in the modeling of polyelectrolytes and complex coacervation. Macromolecules 56(15):5941–5963

Sircar S, Keener JP, Fogelson AL (2013) The effect of divalent vs. monovalent ions on the swelling of mucin-like polyelectrolyte gels: governing equations and equilibrium analysis. J Chem Phys 138(1):014901

Slim AH, Shi WH, Safi Samghabadi F, Faraone A, Marciel AB, Poling-Skutvik R, Conrad JC (2022) Electrostatic repulsion slows relaxations of polyelectrolytes in semidilute solutions. ACS Macro Lett 11(7):854–860

Smiatek J (2020) Theoretical and computational insight into solvent and specific ion effects for polyelectrolytes: the importance of local molecular interactions. Molecules 25(7):1661

Sommer S (2025) Evaluation of carboxymethyl cellulose as an additive for selective protein removal from wine. Fermentation 11(5):273

Spiteri MN (1997) Conformation et arrangement des polyelectrolytes en solution semi-diluee. Etude par diffusion des neutrons aux petits angles. PhD thesis, Paris 11

Strauss UP, Ross PD (1959) Counterion binding by polyelectrolytes. IV. Membrane equilibrium studies of the binding of univalent cations by long-chain polyphosphates1. J Am Chem Soc 81(20):5299–5302

Tang Q, Rubinstein M (2022) Where in the world are condensed counterions? Soft Matter 18(6):1154–1173

Tasaki I (2012) Physiology and electrochemistry of nerve fibers. Elsevier, Amsterdam

Tondre C, Zana R (1971) Ultrasonic absorption as a probe for the study of site binding of counterions in polyelectrolyte solutions. J Phys Chem 75(21):3367–3372

Tondre C, Zana R (1972) Apparent molal volumes of polyelectrolytes in aqueous solutions. J Phys Chem 76(23):3451–3459

Tondre C, Zana R (1975) Comments on letter: 'Dilatometric study of monovalent counter-ion association with polymethacrylate': J. Komiyama, Y. Takeda, M. Ando and T. Iijima, Polymer 1974, 15, 468–470. Polymer 16(3):228–229

Tondre C, Kale K, Zana R (1978) Density and ultrasonic absorption studies of the interaction between polyions and hydrophobic counterions. Eur Polym J 14(2):139–143

Trivedi HC, Patel RD (1986) Studies on carboxymethylcellulose: conductivity measurements of solutions, 2. Die Makromolekulare Chem Macromol Chem Phys 187(1):199–210

Truzzolillo D, Cametti C, Sennato S (2009) Dielectric properties of differently flexible polyions: a scaling approach. Phys Chem Chem Phys 11(11):1780–1786

Verdugo P (2005) Polymer gel phase transition in condensation–decondensation of secretory products. In: Dušek, K. (eds) Responsive Gels: Volume Transitions II. Advances in Polymer Science, vol 110. Springer, Berlin, Heidelberg

Vlachy N, Jagoda-Cwiklik B, Vácha R, Touraud D, Jungwirth P, Kunz W (2009) Hofmeister series and specific interactions of charged headgroups with aqueous ions. Adv Coll Interface Sci 146(1–2):42–47

Wagner P, Różańska S, Warmbier E, Frankiewicz A, Różański J (2023) Rheological properties of sodium carboxymethylcellulose solutions in dihydroxy alcohol/water mixtures. Materials 16(1):418

Wandrey C (1999) Concentration regimes in polyelectrolyte solutions. Langmuir 15(12):4069–4075

Wandrey C, Hunkeler D, Wendler U, Jaeger W (2000) Counterion activity of highly charged strong polyelectrolytes. Macromolecules 33(19):7136–7143

Wang W, Ji S, Xia Q (2024) Influence of carboxymethyl cellulose on the stability, rheology, and curcumin bioaccessibility of high internal phase pickering emulsions. Carbohyd Polym 334:122041

Wnek GE (2016) Perspective: do macromolecules play a role in the mechanisms of nerve stimulation and nervous transmission? J Polym Sci, Part B: Polym Phys 54(1):7–14

Yoshida M, Nakagawa D, Hozumi H, Horikawa Y, Makino S, Nakamura H, Shikata T (2024) A new concept for interpretation of the viscoelastic behavior of aqueous sodium carboxymethyl cellulose systems. Biomacromol 25(6):3420–3431

Zana R (1975) Studies of aqueous solutions of polyelectrolytes by means of ultrasonic methods. J Macromol Sci Rev Macromol Chem 12(2):165–189

Zana R, Tondre C (1975a) Ultrasonic studies of polyion polyelectrolytes solutions. In: Chemical and biological applications of relaxation spectrometry: proceedings of the NATO Advanced Study Institute Held at the University of Salford, Salford, England, 29 August–12 September, 1974, 18:333

Zana R, Tondre C (1975b) Ultrasonic studies of polyion—counterion interactions in polyelectrolytes solutions. In: Chemical and Biological Applications of Relaxation Spectrometry: Proceedings of the NATO Advanced Study Institute held at the University of Salford, Salford, England, 29 August–12 September, 1974. Springer, pp 333–341

Zana R, Tondre C, Rinaudo M, Milas M (1971) Étude ultrasonore de la fixation sur site des ions alcalins sur des carboxymethylcelluloses de densité de charge variable. J Chim Phys 68:1258–1266

Zhang Y, Douglas JF, Ermi BD, Amis EJ (2001) Influence of counterion valency on the scattering properties of highly charged polyelectrolyte solutions. J Chem Phys 114(7):3299–3313

Zhang W, Liu Y, Xuan Y, Zhang S (2022) Synthesis and applications of carboxymethyl cellulose hydrogels. Gels 8(9):529

Zhang M, Xu T, Zhao Q, Liu K, Liang D, Si C (2024) Cellulose-based materials for carbon capture and conversion. Carbon Capture Sci Technol 10:100157

Publisher's Note Springer Nature remains neutral with regard to jurisdictional claims in published maps and institutional affiliations.